

## ON FLYING THROUGH THE BASE OF A PSEUDO-STREAMER

F.S. Mozer <sup>1,2</sup>, O. V. Agapitov<sup>1</sup>, K.-E. Choi<sup>1</sup>, A. Voshchepynets<sup>3</sup>

<sup>1</sup>Space Sciences Laboratory, University of California, Berkeley, 94720, USA.

<sup>2</sup>Physics Department, University of California, Berkeley, 94720, USA.

<sup>3</sup>Dept. of System Analysis and Optimization Theory, Uzhhorod National University, Uzhhorod, Ukraine.

### ABSTRACT

Near the 10 solar radius perihelion of Parker Solar Probe orbit 24, a confined region containing an enhanced plasma density ( $25,000 \text{ cm}^{-3}$ ) and broadband electrostatic waves was encountered. The solar wind velocity (200 km/sec) and ion temperature (25 eV) were significantly reduced as compared to their values in the ambient solar wind. These anomalous plasma conditions were observed on closed magnetic field lines, as determined from observations of the suprathermal electron strahl. Because the polarity of the radial magnetic field did not change sign on the two sides of the crossing and the crossed region contained a double-peaked plasma structure, the spacecraft must have passed through the base of a pseudo-streamer whose structure extended out to 10 solar radii. In the plasma frame, an electric field as large as 400 mV/m was detected during the crossing. The current associated with this electric field was less than  $1 \text{ mA/m}^2$ , corresponding to a drift velocity less than 2.5 km/sec. It also contained a turbulent plasma with density fluctuations,  $(\Delta n/n)$ , as large as 0.3, suggesting that the resistive term in the Generalized Ohm's Law (GOL) was significant. Also, the density as a function of time had a non-zero slope when the electric field was non-zero, suggesting that the pressure gradient term in the GOL also mattered. As compared to earlier remote sensing and theoretical results, it is surprising that the plasma in this pseudo-streamer had a remarkably low flow velocity and that the pseudo-streamer base extended out to 10 solar radii.

### INTRODUCTION

Coronal streamers are detected frequently in remote observations of the solar corona. They are confined spatial structures containing enhanced plasma densities, slow solar wind, and cold perpendicular ions [Koutchmy, 1995; Morgan and Cook, 2020]. Coronal streamers fall into two primary topological categories: helmet streamers (or bipolar streamers) and pseudo-streamers (or unipolar streamers). The distinction is defined by the magnetic polarity of the adjacent coronal regions. Helmet streamers separate coronal regions of opposite polarity and are characterized by a large sheet of closed, trans-equatorial magnetic field lines that ultimately form the Heliospheric Current Sheet (HCS) beyond the Sun (Wilcox and Ness, 1965; Wang & Sheeley Jr, 2007; Owens et al., 2013).

In contrast, pseudo-streamers separate coronal regions of the same magnetic polarity and do not feature a heliospheric current sheet (Wang et al., 2019; Abbo et al., 2016). This fundamental difference in magnetic structure leads to distinct plasma properties and solar wind characteristics.

Pseudo-streamer plasma sheets tend to exhibit lower internal electron densities and are generally described as being more quiescent than helmet streamers, showing a steady outflow without the characteristic density spikes or plasma blobs associated with helmet streamer activity (Wang & Sheeley Jr, 2007; Wang et al., 2012; Abbo et al., 2015). Furthermore, while helmet streamers are unambiguously linked to the slowest component of the solar wind, pseudo-streamers are typically associated with wind speeds in the intermediate range, spanning from approximately 320 to 600 km/s (Wang et al., 2019; Wang et al., 2012; Wallace et al., 2020). The precise contribution of these structures to solar wind acceleration is crucial, as they are known to possess multiple topological elements that enable energy release through interchange reconnection (Pellegrin-Frachon et al., 2023; Owens et al., 2013). This relationship between pseudo-streamers and the large-scale solar wind structure for the event described in this paper has been presented [Bale et al, 2025].

From the solar surface outward, the parts of a pseudo-streamer consist of a base, a stalk, a topological boundary, and an open field line region. The base is a closed magnetic field line region thought to extend over several solar radii and is the foundation of the structure, consisting of magnetic field lines that loop back down to the Sun's surface. These closed loops hold the dense, hot plasma that creates the bright feature visible in coronal images. Despite their recognized importance as persistent structures, direct, *in situ* measurements deep within the plasma sheet of a pseudo-streamer, particularly near its base in the low corona, have previously been inaccessible. The Parker Solar Probe (PSP), has now reached the inner heliosphere, offering an unprecedented opportunity to fly through these magnetically defined boundaries. Understanding the physical parameters—including the full velocity profile, turbulence characteristics, thermal state, fields and currents—within the region where the transition from closed to open field lines occurs is essential for validating current magnetohydrodynamic (MHD) models and resolving the origin of the slow and intermediate solar wind. In this paper, PSP observations inside the base of a pseudo-streamer are presented. The electric and magnetic field data for this presentation came from the FIELDS instruments [Bale et al, 2016] while the plasma data was produced by the SPAN instruments [Whittlesey et al, 2020]. All data in this paper are presented in the PSP spacecraft frame whose positive Z-direction points sunward.

## DATA

Figure 1 displays Parker Solar Probe measurements near 10 solar radii on orbit 24. Figure 1a shows a 24-hour interval during which there were both broadband and narrowband electric field waves. Over most of the region there were few hundred Hz, narrowband, triggered ion acoustic waves that have been described [Mozer et al, 2021; 2022; 2023; 2025a]. However, during an ~two-hour interval near perihelion there were major changes due to the presence of broadband electrostatic waves. During this time interval, the plasma density of figure 1b was almost an order of magnitude enhanced while the solar wind flow of figure 1c was slow (200 km/sec as compared to a typical solar wind flow greater than 400 km/sec) and the perpendicular ion temperature of figure 1d was a factor of more than two lower than in the typical solar wind. The radial-component of the magnetic field, illustrated in

figure 1e, was positive on both sides of the region of interest and had a brief negative excursion during the large density interval. The 1166 eV electron pitch angle distribution (the high energy component of the electron suprathermal population) in figure 1f had a beam-like distribution near  $180^\circ$ , which means that the electron beam flowed opposite to the direction of the magnetic field or away from the Sun.

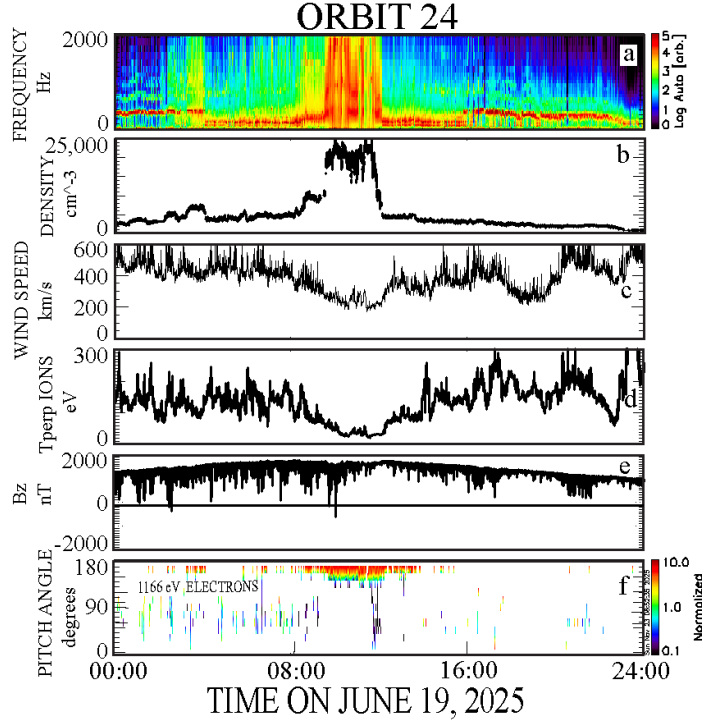


Figure 1. Figure 1a gives the spectrum of the electric field near the Parker Solar Probe perihelion of 10 solar radii. Figure 1b, the plasma density, had a major enhancement at the same time and location that the broadband waves of figure 1a appeared. Figure 1c shows that these structures appeared in a slow solar wind and figure 1d shows that the ion perpendicular temperature was low at this time. Figure 1e shows that the radial component of the magnetic field had the same orientation on both sides and through the event except for a short time interval during the event. Figure 1f displays the electron pitch angle distribution at an energy of 1166 eV, which shows that an outflowing beam of keV electrons appeared through the event.

These results suggest that a fixed structure existed for several hours during which the plasma density, waves, etc. built up to produce the observed, spatially confined structure near 10 solar radii. To conclude that the spacecraft passed through the base of a pseudo-streamer during this time interval requires showing that the magnetic field lines were closed. This is the case if there is electron strahl flowing sunward on such field lines. The strahl (narrow, highly collimated beam of suprathermal electrons) is a crucial kinetic diagnostic in the solar wind [Marsh et al, 2006]. Its primary flow direction is essential for inferring the magnetic field's topology. It originates in the

lower solar corona where thermal electrons escape the solar electric potential and become collimated by the rapidly diverging magnetic field. Observing the strahl flowing sunward is evidence that the local magnetic field line is closed and attached to the Sun at both ends [Bruno et al, 2013].

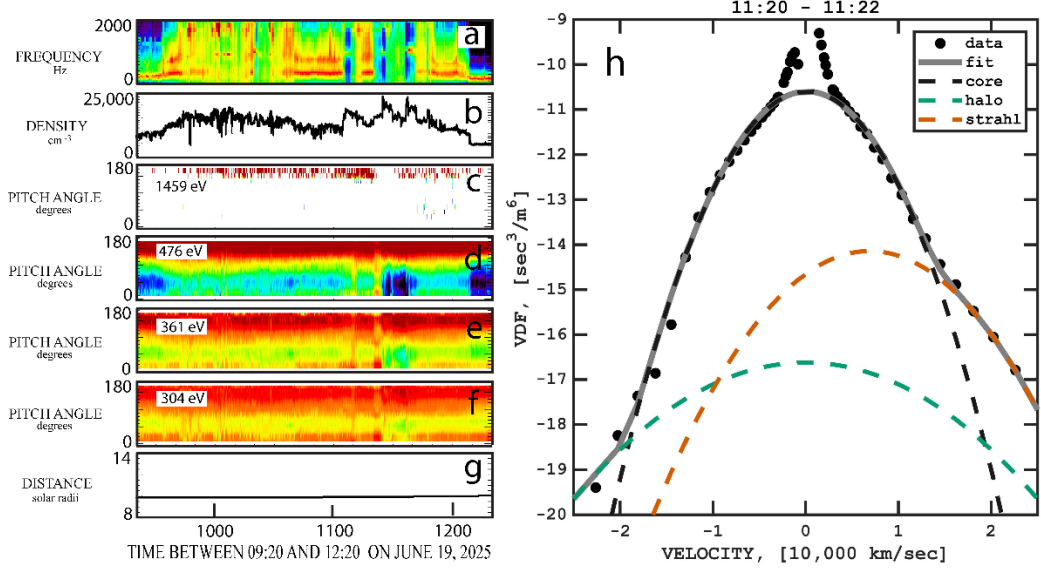


Figure 2. A three hour time interval near the perigee of orbit 24 during which figure 2a presents the electric field wave spectra, figure 2b gives the plasma density, figures 2c, 2d, 2e, and 2f, illustrate the pitch angle distributions of 1439, 476, 361, and 304 eV electrons, while figures 2g gives the spacecraft distance from the center of the Sun in units of solar radii and 2h presents the electron velocity distribution function (eVDF) during a two minute interval. Figures 2e and 2f show that sunward flowing strahl electrons existed while the plasma density was large. This, plus the strahl electron distribution (the red dashed curve of figure 2h), provides the final proof that the field lines were closed at this time.

Figure 2 provides closed field line evidence during the event of interest. Figures 2a through 2g include the approximately three-hour interval during which the plasma density of figure 2b was large. The small pitch angle, sunward propagating electrons in figures 2e and 2f were present through most of the interval. This small pitch angle sunward propagating flux of electrons is strahl that originated at the opposite foot point of the closed field line of interest. The electron VDF during a two-minute interval is presented in figure 2h. The sunward flowing strahl (the red dashed curve in figure 2h) once again proves that the field lines were closed during the interval of interest.

The plasma density shown in figure 1b had a two-peak distribution. This is consistent with and required for a pseudo-streamer, as illustrated by the model of the magnetic field geometry in the pseudo-streamer base in figure 3a. This model also requires a reversal of the radial component of the magnetic field between the two peaks. Examination of figure 1e shows that a narrow, negative,

$B_z$  component (the radial component) was present in the data. This region is zoomed in figures 3b through 3h and a plausible trajectory of the spacecraft through this region is given as the red curve in figure 3a. On this trajectory, the radial-component of the magnetic field, initially positive, goes through zero to become negative, and then returns to being positive through the rest of the trajectory. This is exactly the  $B_z$  behavior illustrated in figure 3d. Additionally, the  $B_y$  component, illustrated in figure 3c, starts small in the model, becomes positive in the vicinity of the negative  $B_z$ , and then returns to zero through the rest of the trajectory. Meanwhile, the plasma density of figure 3e was minimum in the vicinity of the field reversal, as expected from the trapping of the plasma in the double peak distribution. This agreement of the data with the two-peak geometry is remarkable confirmation that the spacecraft passed through the base of a pseudo-streamer.

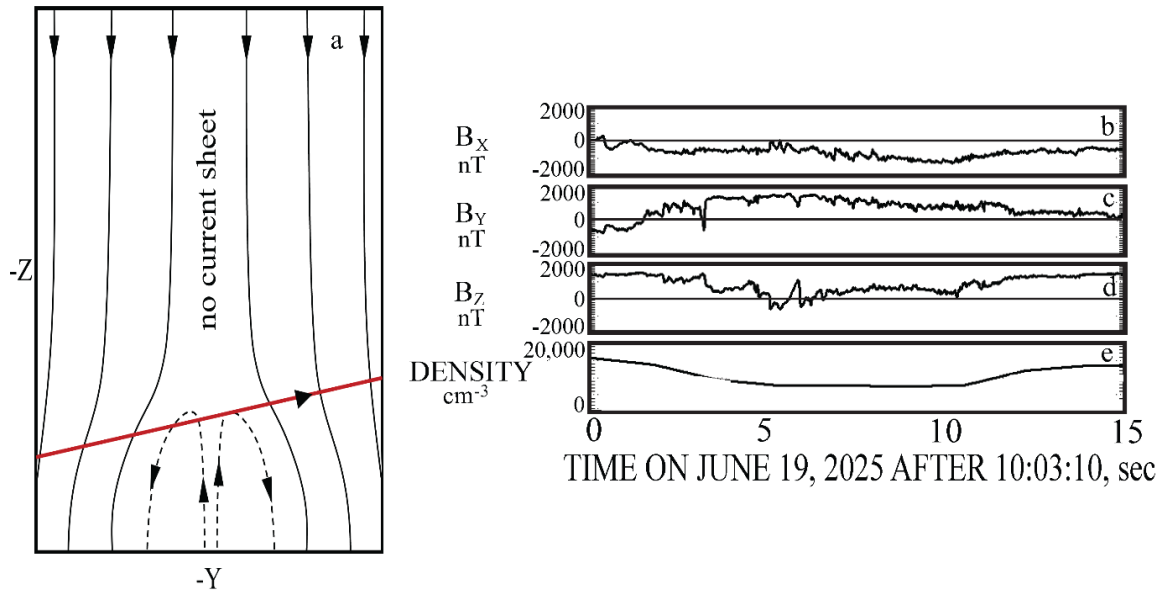


Figure 3. Figure 3a, a model of the magnetic field geometry near a pseudo-streamer, is a modified figure taken from Crooker et al, [2014]. It illustrates the double structure at the base of the pseudo-streamer and shows (in red) a plausible spacecraft trajectory through it. Figures 3b, 3c, and 3d provide the magnetic field components measured on PSP as it crossed the pseudo-streamer, while the plasma density is given in figure 3e.

Given that the spacecraft was inside the base of a pseudo-streamer, it is interesting to examine the electrodynamics of the plasma. To do this, the measured  $E_x$  and  $E_y$  were transformed into the plasma rest frame, defined as the frame in which the ion flow was zero. Additionally, the unmeasured  $E_z$  was found by assuming that the parallel electric field was zero, or that

$$E_Z' = (-E_X' B_X - E_Y' B_Y) / B_Z \quad (1)$$

The electric and magnetic fields in this prime frame are shown in Figure 4 during a 15-minute time interval, with the prime electric field components in figures 4c, 4d, and 4e, while the magnetic field is given in figures 4f, 4g, and 4h.

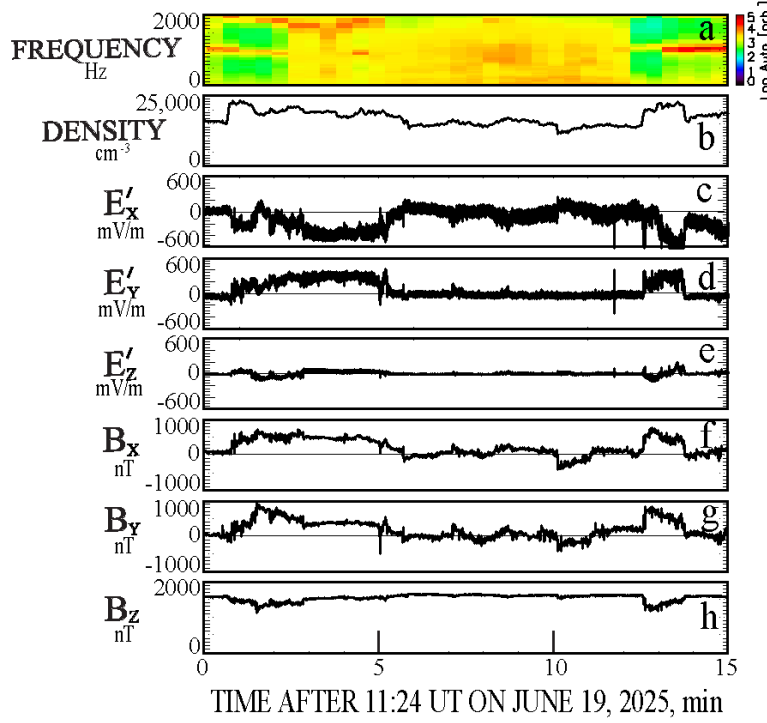


Figure 4. The electric and magnetic fields measured in the plasma frame of rest inside the pseudo-streamer. Figure 4a gives the electric field wave spectrum, figure 4b gives the plasma density, figures 4c, 4d, and 4e give the prime electric field and figures 4f, 4g, and 4h give the magnetic field

The very large electric field in the plasma rest frame may be explained by invoking the Generalized Ohm's Law (GOL), which is

$$\mathbf{E}' = \mathbf{E} + \mathbf{v} \times \mathbf{B} = \eta \mathbf{J} + \mathbf{J} \times \mathbf{B} / ne - \nabla P / ne + (me / ne^2) \partial \mathbf{J} / \partial t \quad (2)$$

where  $\mathbf{v} \times \mathbf{B}$  is less than 20% of  $\mathbf{E}$  and

$\mathbf{v}$  = plasma bulk velocity

$\eta$  = collisional resistivity

$\mathbf{J}$  = current density

$n$  = plasma density

$\nabla P$  = pressure gradient

It is expected that the first three terms on the right side of equation (2) are important inside a pseudo-streamer. The measurements are inadequate for determining any of them, but some limits

may be derived. For example, if the  $\mathbf{J} \times \mathbf{B}/ne$  term dominated the other terms on the right side of the equation, the current density would be about 1 mamp/m<sup>2</sup>. This is an overestimate of the current density when the remaining terms in the GOL are non- zero. That the pressure gradient term may have been non-zero is indicated by the finite slope of the density plot in figure 4b during the time intervals (one near the beginning and one near the end of figures 4c and 4d) when the electric field was non-zero. That the resistivity term may also have been non-zero is shown by the figure 5b plot in which the relative density fluctuations,  $\Delta n/n$ , (the density fluctuations divided by the average density) are relatively large inside the pseudo-streamer base when the density of figure 5a was large. The relative density is obtained from the spacecraft potential converted into a high time resolution measurement of the plasma density and its fluctuations [Mozer et al, 2022a].

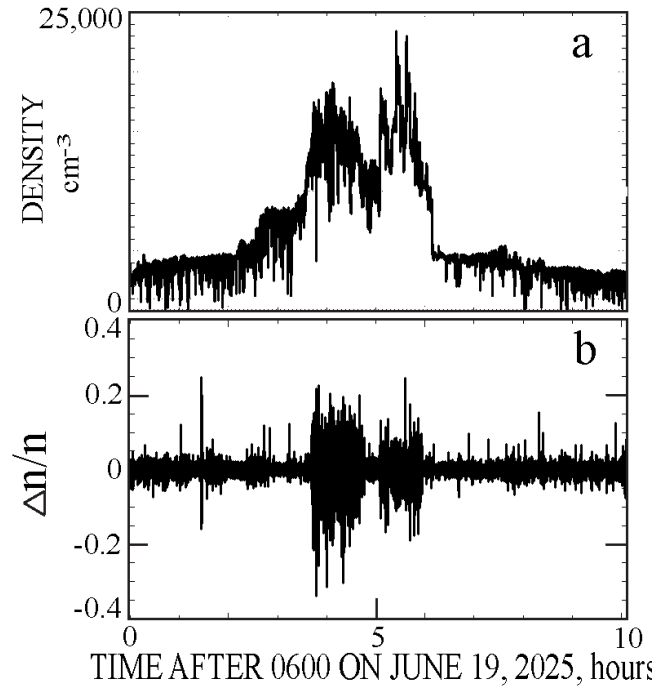


Figure 5. Figure 5a presents the density measured inside and around the pseudo-streamer. Figure 5b presents  $\Delta n/n$ , the density fluctuations divided by the average density. That the density fluctuations were large shows that the plasma was turbulent.

## SUMMARY

1. The Parker Solar Probe traversed the base of a coronal pseudo-streamer at 10 solar radii. The pseudo-streamer identification is confirmed by three key observations: (i) a double-peaked electron density structure (peak density  $\sim 25,000 \text{ cm}^{-3}$ ), (ii) situated on closed magnetic field lines, and (iii) invariant magnetic field polarity across the structure.
2. That the pseudo-streamer base extended to 10 solar radii, that the plasma speed was as small as 200 km/sec, and that the perpendicular and parallel ion temperatures were as small as 25 eV, all differ from expectations based on remote sensing and existing models.
3. In the plasma rest frame, electric fields as large as 400 mV/m were observed.
4. If this electric field was largely supported by the  $\mathbf{J} \times \mathbf{B}/ne$  term in the Generalized Ohm's Law, current densities as large as 1 mA/m<sup>2</sup>, associated with drift velocities of 2.5 km/sec, must have been present.

5. The above estimates represent an upper bound, as they neglect contributions from the resistive term ( $\eta J$ ) and pressure gradient term ( $-\nabla P_e/n_e$ ) in the Generalized Ohm's Law. These terms must be non-negligible, given that normalized density fluctuations ( $\Delta n/n$ ) reached values as high as 0.3, and the slope of the density curve was non-zero when the electric field was large.

## ACKNOWLEDGEMENTS

This work was supported by NASA contract NNN06AA01C. The authors acknowledge the extraordinary contributions of the Parker Solar Probe spacecraft engineering team at the Applied Physics Laboratory at Johns Hopkins University. The FIELDS experiment on the Parker Solar Probe was designed and developed under NASA contract NNN06AA01C. OVA was supported by NASA contracts 80NSSC22K0433, 80NNSC19K0848, 80NSSC21K1770, and NASA's Living with a Star (LWS) program (contract 80NSSC20K0218).

## REFERENCES

Abbo, L., Lionello, R., Riley, P., & Wang, Y. M. (2015). Coronal pseudo-streamer and bipolar streamer observed by SOHO/UVCS in March 2008. *Solar Physics*, 290(7), 1957–1975.

Abbo, L., Ofman, L., Antiochos, S. K., Hansteen, V. H., & Ko, Y.-K. (2016). Slow solar wind: observations and modeling. *Space Science Reviews*, 201(1), 1–66.

Bale, S.D., Goetz, K., Harvey, P.R., Turin, P. Bonnell, J.W., et al, (2016) “The Fields Instrument Suite for Solar Probe Plus”, SSRv, 204, 49

Bale, S.D., Al Nussirat, S., Badman, S., Drake, J., Eastwood, J. et al [2025] In situ measurement of reconnection jets from a pseudostreamer complex, SH31A-07, Fall meeting AGU

Bruno, R., Carbone, V. (2013) The Solar Wind as a Turbulence Laboratory. *Living Rev. Sol. Phys.* **10**, 2, <https://doi.org/10.12942/lrsp-2013-2>

Crooker, N. U., McPherron, R.L., and Owens, M.J. (2014), Comparison of interplanetary signatures of streamers and pseudostreamers, *J. Geophys. Res. Space Physics*, 119, 4157–4163, doi:10.1002/2014JA020079

Koutchmy, S. (2005) Coronal Streamers, Encyclopedia of Astronomy & Astrophysics P. Murdin © IOP Publishing Ltd 2005 ISBN: 0333750888, DOI: 10.1888/0333750888/2271

Marsch, E., (2006) Kinetic Physics of the Solar Corona and Solar Wind. *Living Rev. Sol. Phys.* **3**, 1. <https://doi.org/10.12942/lrsp-2006-1>

Morgan, H. and Cook, A.C. (2020) The Width, Density, and Outflow of Solar Coronal Streamers, *The Astrophysical Journal*, 893:57 <https://doi.org/10.3847/1538-4357/ab7e32>

Mozer, F. S., Bale, S. D., Cattell, C. A., et al, (2021). Triggered ion acoustic waves in the solar wind. *Physical Review Letters*, 127(8), 085101.

Mozer, F. S., Bale, S. D., Cattell, C. A., et al (2022). Core Electron Heating By Triggered Ion Acoustic Waves, *The Astrophysical Journal Letters*, 927:L15, <https://doi.org/10.3847/2041-8213/ac5520>

Mozer, F.S., Bale, S.D., Kellogg, P.J., Larson, D., Livi, R., and Romeo, O. (2022a), An Improved Technique for Measuring Plasma Density to High Frequencies on the Parker Solar Probe, *The Astrophysical Journal*, 926:220, <https://doi.org/10.3847/1538-4357/ac4f42>

Mozer, F.S., Bale, S.D., Kellogg, P.J. et al, (2023) Arguments for the physical nature of the triggered ion-acoustic waves observed on the Parker Solar Probe, *Phys. Plasmas* 30, 062111 doi: 10.1063/5.0151423

Mozer, F.S., Agapitov, O.V., Choi, K-E., et al, (2025a) Parallel Electric Fields and Electron Heating Observed in the Young Solar Wind, *The Astrophysical Journal*, 981:82 <https://doi.org/10.3847/1538-4357/adb582>

Mozer, F.S., Voshchepynets, A., Agapitov, O.V., Choi, K.-E., Colomban, L., Sydora, R., (2025b), Intermingled open and closed magnetic field lines near the radial origin of the heliospheric current sheet. *The Astrophysical Journal*, 979(1), 16.DOI: <https://doi.org/10.3847/1538-4357/ad9a77>

Owens, M. J., Crooker, N. U., & Schwadron, N. A. (2013). Solar origin of heliospheric magnetic field inversions: Evidence for coronal loop opening within pseudostreamers. *Journal of Geophysical Research: Space Physics*, 118(2), 527–543.

Pellegrin-Frachon, T., Masson, S., Pariat, É., Abbo, L., & Riley, P. (2023). Interchange reconnection dynamics in a solar coronal pseudo-streamer. *Astronomy & Astrophysics*, 673, A131.

Riley, P., Luhmann, J.G. (2012). Interplanetary Signatures of Unipolar Streamers and the Origin of the Slow Solar Wind. *Sol Phys* 277, 355–373 <https://doi.org/10.1007/s11207-011-9909-0>

Schatten, K. H., Wilcox, J. M., & Ness, N. F. (1969). A model of interplanetary and coronal magnetic fields. *Solar Physics*, 6, 442–455.

Wallace, S., Arge, C. N., Viall, N., Thompson, S. L., & DeForest, C. E. (2020). On the relationship between magnetic expansion factor and observed speed of the solar wind from coronal pseudostreamers. *The Astrophysical Journal*, 898(1), 36.

Wang, Y. M., Grappin, R., Robbrecht, E., & Sheeley Jr, N. R. (2012). On the nature of the solar wind from coronal pseudostreamers. *The Astrophysical Journal*, 749(1), 84.

Wang, Y. M., & Panasenco, O. (2019). Observations of solar wind from earth-directed coronal pseudostreamers. *The Astrophysical Journal*, 882(1), 36.

Wang, Y. M., & Sheeley Jr, N. R. (2007). Coronal pseudostreamers. *The Astrophysical Journal*, 659(1), 754–759.

Whittlesey, P.L., Larson, D.E., Kasper, J.C. Halekas, J., Abatcha, M., et al, (2020) The Solar Probe ANalyzers—Electrons on the Parker Solar Probe, *The Astrophysical Journal Supplement Series*, 246:74 (14pp), February <https://doi.org/10.3847/1538-4365/ab7370>

Wilcox, J.M., and Ness, N.F., (1965), Quasi-stationary corotating structure in the interplanetary medium, *Journal of Geophysical Research*, 70, <https://doi.org/10.1029/JZ070i023p05793>